Journal of Communications and Information Networks, Vol.2, No.2, Jun. 2017
DOI: 10.1007/s41650-017-0024-8

Research paper

Special Issue on Internet of Vehicle

Network capacity analysis for cellular based cognitive radio VANET in urban grid scenario

Xinxin He[1*], Hang Zhang[1], Tao Luo[1], Weisen Shi[2]

1. Beijing Laboratory of Advanced Information Networks, Beijing University of Posts and Telecommunications, Beijing 100876, China
2. Department of Electrical and Computer Engineering, University of Waterloo, Waterloo ON N2L 3G1, Canada

* Corresponding author, Email: hxx_9000@bupt.edu.cn

Abstract: The spectrum scarcity of VANETs (Vehicular Ad hoc Networks) can be alleviated by spectrum sharing technology. We present a framework of CCR-VANETs (Cellular-based Cognitive-radio Vehicular Ad hoc Networks). In CCR-VANETs, cellular network performs as primary network while VANET shares the downlink spectrum of cellular network. We consider a scalable urban grid scenario in which vehicles detect available spectrum holes and opportunistically access them according to a carrier-sensing multiple-access protocol. To restrict vehicles' interference to primary receivers, we set a square preservation region around each particular street block where an active base station is located. The number of street blocks in the preservation region is calculated with the practical assumption that vehicles only know the locations of primary transmitters. We analyze the aggregate interference power from primary and secondary networks, then derive the lower-bound of downlink capacity for the primary network and lower-bound of V2V (Vehicle-to-Vehicle) channel capacity for the secondary network respectively. The numerical results demonstrate the impacts of different network parameters on inter-networks interference level and network capacities.

Keywords: cognitive radio, VANET, cellular networks, CSMA, network capacity

Citation: X. X. He, H. Zhang, T. Luo, et al. Network capacity analysis for cellular based cognitive radio VANET in urban grid scenario [J]. Journal of communications and information networks, 2017, 2(2): 136-146.

1 Introduction

Vehicular Ad hoc network, which merges informatics technologies and wireless communications into transportation system, has become an important research topic followed by academia, industries, and governments. In VANET, vehicles equipped with onboard sensors and control systems generate data and disseminate it among other vehicles through DSRC (Dedicated Short Range Communications) protocol[1]. Various services can be carried on VANET including safety applications (collision detection, congestion information, lane change warning, etc.) and entertainments applications (mobile office, Internet access, multimedia transmission, etc.)[2]. With the increasing demands of bandwidth resources to support emerging applications, the 75 MHz DSRC band between 5.850 and 5.925 GHz is proved to be insufficient[3,4]. Alleviating the spectrum scarcity of VANET is an urgent issue[5].

CR (Cognitive Radio) is a promising approach to deal with spectrum scarcity, which enables unli-

Manuscript received Feb. 23, 2017; accepted Apr. 01, 2017
This work is supported in part by the National Natural Science Foundation of China (Nos. 61271184, 61571065).

censed users to opportunistically exploit the spectrum of licensed users[6,7]. Considering the challenge faced by VANET, cognitive radio is introduced into VANETs to solve spectrum scarcity and form CR-VANETs (Cognitive Radio VAENT)[8]. Vehicles in CR-VANETs can opportunistically exploit the licensed spectrum without interfering primary users. In Ref. [9], Felice et al. proposed a novel spectrum management framework for CR-VANETs, which allows vehicles to opportunistically access spectrum holes in ultra-high frequency TV bands. In Ref. [10], Fawaz et al. proposed a system that extends the spectrum allocated for VANET control messages into TV spectrum. However, for some vital applications in VANET, it is difficult to ensure QoS requirements when transmitting their data through TV spectrum with a cognitive radio method[11,12]. Beside the TV spectrum, cellular networks are introduced to carry out vehicular applications by many works, such as LTE-V technology[13]. In Ref. [14], Kim et al. present a scenario for CR networks, in which secondary users transmit signals in downlink channels of cellular network with a pre-defined interference temperature limit. In Ref. [15], Feizi et al. proposed an efficient model for a mobile Ad hoc network that opportunistically exploits the idle channels in the cellular network. Besides, a new type of cellular network service connecting buses with base stations to provide free Wi-Fi on buses has been adopted in many countries[16]. With dedicated base stations and cellular network resources allocated to bus Wi-Fi, it is possible to opportunistically use them to enhance VANET communications. These contributions motivated us to consider a system sharing downlink spectrum of a bus Wi-Fi cellular network with VANET.

Numerous studies have investigated spectrum sensing and allocation in CR-VANETs, while few of them focusing on network capacity. In Ref. [17], Gupta and Kumar investigated the capacity of wireless Ad hoc networks. In Ref. [18], Weber et al. introduced transmission capacity, which is defined as the product of the maximum density of successful transmissions and the corresponding data rate, with a constraint on outage probability. Recent studies made efforts toward capacity performance analysis of traditional large-scale CR networks under geometry frameworks. In Ref. [19], Yin et al. investigated the transmission capacities of two overlaid mobile networks. In Ref. [20], Huang et al. studied spectrum sharing between a cellular network and a mobile cognitive Ad hoc network, and analyzed the transmission capacity performance trade-off between them. Due to some unique characteristics, results achieved in Ad hoc network research cannot be directly applied to VANET. For instance, network topologies in Ad hoc networks are described as random distributions on a two-dimensional plane, while in VANET research, since vehicles' mobility is limited by roads, topologies are modeled as one-dimensional lines or grids. Maintaining a long-lasting unicast communication flow among vehicles over a long distance is unnecessary because VANETs are mainly involved in proximity related applications, such as localized social content sharing and safety message dissemination. In Ref. [21], Jacquet et al. analyzed asymptotic bounds of VANET capacity in a straight road scenario but ignored the effect of interference. Lu et al. investigated the asymptotic throughput capacity of a social-proximity VANET in a downtown grid scenario[22], and studied the capacity-cost tradeoffs for vehicular access networks[23]. The downlink capacity of vehicles has been lower-bounded by considering a perfect city grid with the distribution of nodes following a Poisson point process.

In this paper, we investigate the capacity of CCR-VANETs (Cellular-based Cognitive-Radio VANETs) with CSMA (Carrier-Sensing Multiple-Access) protocol. The CCR-VANETs system is shown in Fig. 1. The main contributions of this study are as follows:

• The theoretical capacity of the CCR-VANETs in urban grid scenario is proposed. We study the downlink spectrum sharing between a bus Wi-Fi cellular network and VANET. Vehicles opportunistically access the downlink spectrum of the primary network by exploiting available spectrum holes.

• To keep an acceptable level of interference to primary receivers, we set a square preservation region which contains appropriate street blocks around a particular street block where a base station is located. The number of street blocks is discussed with the practical assumption that the vehicles know only the locations of primary transmitters.

• With the analysis of aggregate interference power from the primary and secondary networks, we obtain the lower-bound of base station-to-bus downlink transmission capacity for primary network, and lower-bound of V2V transmission capacity for secondary network.

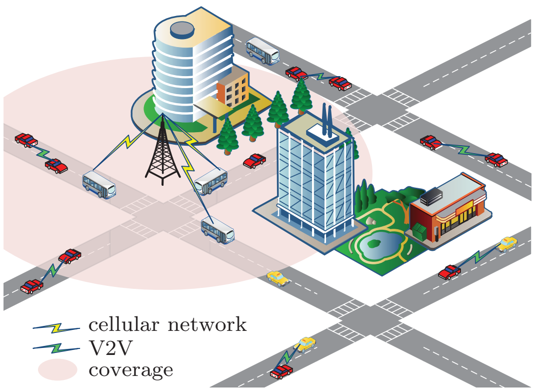

Figure 1 CCR-VANETs System

The rest of this paper is organized as follows. The system model and definitions are described in section 2. The capacities of primary and secondary networks are analyzed in section 3. The numerical results are presented in section 4. Finally, section 5 gives our conclusions.

2 System model

2.1 Urban street pattern

According to many cities, such as Manhattan and Portland, the street pattern is very common modeled as a grid-like layout[24]. As shown in Fig. 2, the urban geographic area in this paper is modeled by a perfect grid $G(M,L)$, which includes a set of M vertical roads. Each road segment is represented by a line segment of length L, and the total number of road segments is denoted by $g=2(M-1)^2$. In this model, the scale of the urban grid can be characterized by M and L. For instance, M is roughly 100, and L is generally from 80 to 200 m for the downtown area of Toronto[25]. Meanwhile, in order to eliminate the border effects, the urban grid G is considered as a torus of unit area, which is a common practice to avoid tedious technicalities[26].

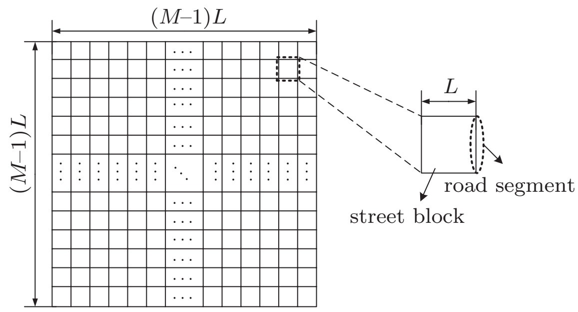

Figure 2 Grid-like urban street pattern

2.2 Node distribution and communication model

In the primary network, considering the downlink, the transmitters are base stations and the receivers are buses. The transmission power of each base station is assumed the same and denoted by P_{p}. We divide the urban grid $G(M,L)$ into N_A squares of equal area A, as shown in upper part of Fig. 3, where N_A is the number of base stations. It can be derived that $|A|=(M-1)^2L^2\big/N_A$, and $N_A<(M-1)^2$. There is one base station placed in the central street block of each square, and each square is composed of multiple tiers that are co-centered at the base station. The base station is located at the street block $Tier\,(1)$, and the adjacent street blocks surrounding $Tier\,(1)$ from $Tier\,(2)$, and so forth. The width of each tier is r and the total number of tiers of each square is denoted by τ_b. The coverage of the cellular is often considered as a hexagon region. For simplicity, it is assumed that the coverage of the base station is a square area of τ_c tiers according to the similar approximation. In Ref. [27]. The direct transmission range of the base station is denoted by $R=(\tau_c-1/2)\,L$. In this paper, we assume $\tau_c<\tau_b$, i.e., the network is partially covered by base stations. As shown in Fig. 3. the yellow square composed by four tiers denotes the direct transmission coverage of the base station, while the green tier and other tiers outside it cannot support direct transmission between cellular users and base station.

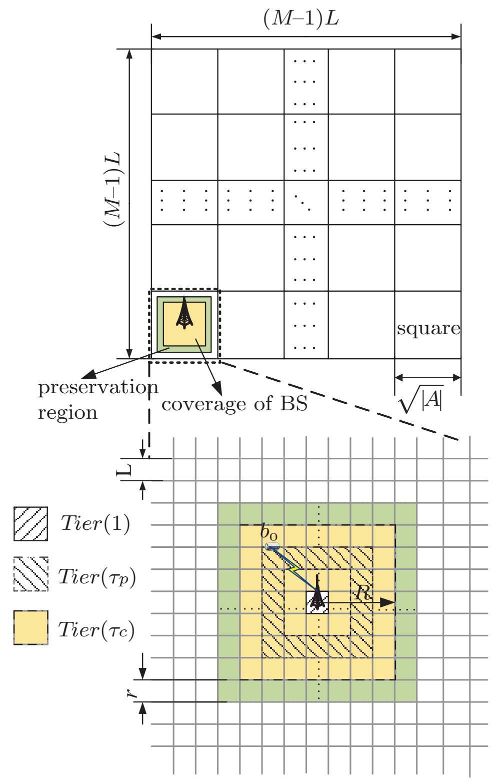

Figure 3 Grid-like VANETs

In the secondary network, we mainly consider the V2V communications. The vehicle opportunistically accesses the licensed spectrum as keeping its interference to the primary network at an acceptable level. We set a preservation region as a square containing K^2 street blocks around a particular street block of the square in which a base station is located. The value of K will be discussed in Section 3. In the preservation regions no vehicles are allowed to transmit. As taking a snapshot of the grid with moving vehicles, the distribution of the vehicles is considered follow a P.P.P. (Poisson Point Process) of density λ. As such, the average number of vehicles in the grid is given as $N = \lambda gL$. Then,

$$\lambda = N/gL = N\Big/2L(M-1)^2. \tag{1}$$

Since λ is positive and bounded, we have $M = \Theta\left(\sqrt{N}\right)$. The transmission power and transmission radius of each communication is assumed the same and denoted by P_s and r, respectively. In V2V transmissions, the CSMA with a carrier sensing radius of $2r$ is adopted to access the spectrum. In other words, the transmitters cannot be active within a distance of $2r$ simultaneously under the CSMA scheme. Therefore, the distribution of active transmitters in the area outside the preservation regions of base stations follows a MHC (Matérn Hard-Core Point Process)[28].

2.3 Channel capacity

For the wireless channel, in this work we ignore the effects of shadowing and small-scale multipath fading and only consider the large-scale path loss, since a macroscopic description of power attenuation previously shown is sufficient for throughput analysis of a long-term average. As such, the received signal power P_{ij} at receiver j from transmitter i is described as follows

$$P_{ij} = \frac{BP_i}{{d_{ij}}^{\alpha}}, \tag{2}$$

where B is a system-dependent constant, P_i is the transmission power of transmitter i, d_{ij} is the transmission distance of transmitter i and the corresponding receiver j, and the path loss exponent α is positive, and $\alpha > 2$. In the following discussion, we normalize B to be unity for simplicity.

The channel capacity of transmitter i and the corresponding receiver j is given by Shannon capacity, i.e.,

$$C_{ij} = W_{ij}\text{lb}\left(1 + SINR_{ij}\right), \tag{3}$$

where $SINR_{ij}$ is the signal-to-interference-plus-noise ratio at receiver j, and W_{ij} is the spectrum bandwidth for the transmission. The interference received at receiver j is the aggregation signal power received from all simultaneous transmitters. What makes our model different from the network models in Refs. [22] and [23] is that we introduce two coexisting networks share downlink spectrum of the cellular network, and set a square preservation region around each primary receiver for keeping influence of interference at an acceptable level.

3 Capacity analysis for the primary and secondary networks

In this section, we derive lower bounds of capacity for the primary network and secondary network respectively. The derivation is mostly based on geometric considerations about interference patterns.

3.1 Capacity analysis for the primary network

In Fig. 3, the bus b_0 is assumed on a road segment of $Tier\,(\tau_p)$ from its base station in the square S_0, where $\tau_p \leqslant \tau_c$. The received signal power of bus b_0 from its own base station is denoted by $P_{\rm pr}$, from the propagation model, we have

$$P_{\rm pr} \geqslant \frac{P_{\rm p}}{(\sqrt{2}R)^{\alpha}} = \frac{P_{\rm p}}{\left[\sqrt{2}L\left(\tau_c - \frac{1}{2}\right)\right]^{\alpha}}, \tag{4}$$

where $P_{\rm p}$ is the transmission power of each base station. Assume all base stations are working simultaneously, let $I_{\rm pp}$ denote the interference generating from all other base stations in the primary network suffered by b_0, we have

$$\begin{aligned} & I_{\rm pp} \\ & \leqslant \sum_{q=1}^{\infty} 8q \frac{P_{\rm p}}{(q\sqrt{|A|} - R)^{\alpha}} \\ & \leqslant 8P_{\rm p}\left[\frac{1}{(}\sqrt{|A|} - R)^{\alpha}\right. \\ & \quad \left. + \int_1^{\infty} \frac{1}{(}\sqrt{|A|}q - R)^{\alpha-1}{\rm d}q\right] \\ & = 8P_{\rm p}\left[\frac{1}{(\sqrt{|A|} - R)^{\alpha}}\right. \\ & \quad \left. + \frac{1}{\sqrt{|A|}(\alpha-2)(\sqrt{|A|} - R)^{\alpha-2}}\right] \\ & = \frac{8P_{\rm p}}{\left(\frac{(M-1)}{{N_A}^{1/2}} - \tau_c + \frac{1}{2}\right)^{\alpha} L^{\alpha}} \\ & \quad \cdot \left[1 + \frac{\left(\frac{(M-1)}{{N_A}^{1/2}} - \tau_c + \frac{1}{2}\right)^2 L{N_A}^{1/2}}{(M-1)(\alpha-2)}\right]. \end{aligned} \tag{5}$$

Now, we discuss the size for the preservation region, i.e., the value of K. Considering the fact that the base station transmits to buses in its effective transmission region, the preservation region should accommodate at least $(2\tau_c - 1)^2$ street blocks to protect the potential buses. Since the buses may be located close to the outer boundary of the coverage of the base station, another layer of protective street block should be added, as shown in Fig. 4.

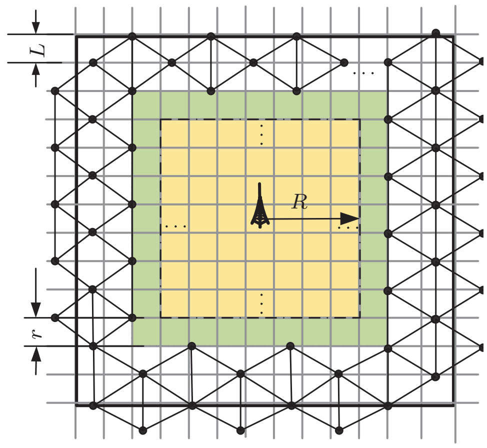

Figure 4 Densest simultaneous transmitters in the secondary network

In this paper, we assume $r = nL$ for simplicity but without loss of generality, where n is an even number. As such, any active vehicles are at least a certain distance away from the potential buses. Therefore, the side length of the preservation square region is defined as

$$KL \geqslant (2\tau_c - 1)\,L + 2nL. \tag{6}$$

Therefore, the minimum value of K is $2\tau_c - 1 + 2n$. In the VANET, we consider a high-density urban environment. Under the CSMA scheme, simultaneous V2V transmitters with carrier sensing radius $2r$ cannot be denser than a triangular lattice[29]. As shown in Fig. 4, due to the preservation region and the CSMA scheme, in the first layer the number of interferers in the secondary network is calculated as

$$c_1 = 4 \cdot \frac{2R + 2r}{2r} = 4\frac{R}{r} + 4. \tag{7}$$

Accordingly, the maximum value of c_1 is $4R/r + 4$. The next $4R/r + 4 \times 2$ interferers form the second layer, and so on, in the qth layer the number of interferers c_q is $4R/r + 4 \times q$. The distance between the receiver marked and interferers in the qth layer is denoted by d_q, and $d_q \in [qL, 2R + qL]$, where $R = (\tau_c - 1/2)\, L$.

The aggregate interference power suffered by b_0 from the secondary network is denoted by $I_{\rm sp}$. Since the close form expression of $I_{\rm sp}$ is difficult to determine, we derive an upper bound of it in the following.

$$\begin{aligned} & I_{\rm sp} \\ & \leqslant \frac{P_{\rm s}}{r^\alpha} \sum_{q=1}^{\infty} \left[\frac{1}{[(q-1)\sqrt{3}+1]^\alpha} \right. \\ & \quad \left. + \frac{1}{\left[(q-1)\sqrt{3}+\delta+1\right]^\alpha} \right] (\delta + 2q) \\ & \leqslant \frac{P_{\rm s}\delta}{r^\alpha} \left[1 + \int_1^\infty \frac{1}{\left[\sqrt{3}q+1-\sqrt{3}\right]^\alpha} {\rm d}q \right] \\ & \quad + \frac{2P_{\rm s}}{r^\alpha} \left[1 + \int_1^\infty \frac{1}{\left[\sqrt{3}q+1-\sqrt{3}\right]^{\alpha-1}} {\rm d}q \right] \\ & \quad + \frac{P_{\rm s}\delta}{r^\alpha} \left[\frac{1}{(\delta+1)^\alpha} \right. \\ & \quad \left. + \int_1^\infty \frac{1}{\left[\sqrt{3}q+\delta+1-\sqrt{3}\right]^\alpha} {\rm d}q \right] \\ & \quad + \frac{2P_{\rm s}}{r^\alpha} \left[\frac{1}{(q+1)^\alpha} \right. \\ & \quad \left. + \int_1^\infty \frac{1}{\left[\sqrt{3}q+\delta+1-\sqrt{3}\right]^{\alpha-1}} {\rm d}q \right] \\ & = \frac{\delta P_{\rm s}}{r^\alpha} \left[1 + \frac{1}{\sqrt{3}\,(\alpha-1)\left(\sqrt{3}q+1-\sqrt{3}\right)^{\alpha-1}} \right] \\ & \quad + \frac{2P_{\rm s}}{r^\alpha} \left[1 + \frac{1}{\sqrt{3}\,(\alpha-2)\left(\sqrt{3}q+1-\sqrt{3}\right)^{\alpha-2}} \right] \\ & \quad + \frac{\delta P_{\rm s}}{r^\alpha} \left[\frac{1}{(\delta+1)^\alpha} \right. \\ & \quad \left. + \frac{1}{\sqrt{3}(\alpha-1)(\sqrt{3}q+\delta+1-\sqrt{3})^{\alpha-1}} \right] \\ & \quad + \frac{2P_{\rm s}}{r^\alpha} \left[\frac{1}{(\delta+1)^\alpha} \right. \\ & \quad \left. + \frac{1}{\sqrt{3}(\alpha-2)(\sqrt{3}q+\delta+1-\sqrt{3})^{\alpha-2}} \right], \end{aligned} \tag{8}$$

where

$$\delta = \frac{2R}{r} = \frac{2\left(\tau_c - \frac{1}{2}\right)}{k}. \tag{9}$$

Let $SINR_b$ denote the $SINR$ of the received signal at b_0. Since the lower bound of $P_{\rm pr}$ and the upper bounds of $I_{\rm pp}$ and $I_{\rm sp}$ are all obtained, from $SINR_b = P_{\rm pr}/(I_{\rm pp} + I_{\rm sp})$, we can derive the lower bound of the $SINR_b$, which is denoted by $SINR_b{}^{\rm lower}$. The background noise is ignored in this work.

Theorem 1 For the primary network, with the bus b_0 on a road segment of $Tier\,(\tau_p)$, the channel capacity of base station-to-bus transmission is lower-bounded by

$$\begin{aligned} C_{\rm p}{}^{\rm lower} &= W{\rm lb}\left(1 + SINR_b{}^{\rm lower}\right) \\ &= W{\rm lb}\left(1 + \frac{P_{\rm pr}}{I_{\rm pp} + I_{\rm sp}}\right). \end{aligned} \tag{10}$$

3.2 Capacity analysis for the secondary network

In the secondary network, we assume a reference vehicle v_0 is on a road segment of $Tier\,(\tau_s)$, where $\tau_c < \tau_s \leqslant \tau_p$. Let $P_{\rm sr}$ denote the received signal power of v_0 from its corresponding transmitter, we have

$$P_{\rm sr} \geqslant \frac{P_{\rm s}}{r^\alpha} = \frac{P_{\rm s}}{(nL)^\alpha}, \tag{11}$$

where $P_{\rm s}$ is the transmission power of each vehicle. Let $I_{\rm ps}$ denote the interference from the signal power of all the base stations in the primary network suffered by v_0. Considering the preservation region around the base station, we have

$$\begin{aligned} I_{\rm ps} &< \frac{P_{\rm p}}{R^\alpha} + \sum_{q=1}^{\infty} 8q \frac{P_{\rm p}}{\left(q\sqrt{|A|} - R\right)^\alpha} \\ &< \frac{P_{\rm p}}{\left(\tau_c - \frac{1}{2}\right)^\alpha L^\alpha} + \\ & \frac{8P_{\rm p}}{\left(\frac{(M-1)L}{N_A{}^{1/2}} - R\right)^\alpha}\left[1 + \frac{\left[(M-1)L/N_A{}^{1/2} - R\right]^2}{(M-1)L(\alpha-2)/N_A{}^{1/2}}\right]. \end{aligned} \tag{12}$$

For the V2V transmissions, under the stipulation of CSMA, the six nearest interferers in the first layer are at distance $2r$ and the next twelve interferors form the second layer, and so on.

As shown in Fig. 5, the distance between the receiver marked and interferers in the first layer is at least r and at least $\left(\sqrt{3}q - 1\right) r$. Let $I_{\rm ss}$ denote the aggregate interference suffered by v_0 from the signal power of all the vehicles in the V2V transmissions in the secondary network . We have

$$
\begin{aligned}
& I_{\mathrm{ss}} \\
& \leqslant \frac{6P_{\mathrm{s}}}{r^{\alpha}} + \sum_{q=2}^{\infty} 6q \frac{P_{\mathrm{s}}}{\left[\left(\sqrt{3}q-1\right)r\right]^{\alpha}} \\
& \leqslant \frac{6P_{\mathrm{s}}}{r^{\alpha}} + \left[1 + \int_{1}^{\infty} \frac{1}{\left(\sqrt{3}q-1\right)^{\alpha-1}} \mathrm{d}q\right] \\
& = \frac{6P_{\mathrm{s}}}{(nL)^{\alpha}} + \left[1 + \frac{1}{\sqrt{3}\left(\alpha-2\right)\left(\sqrt{3}-1\right)^{\alpha-2}}\right]. \quad (13)
\end{aligned}
$$

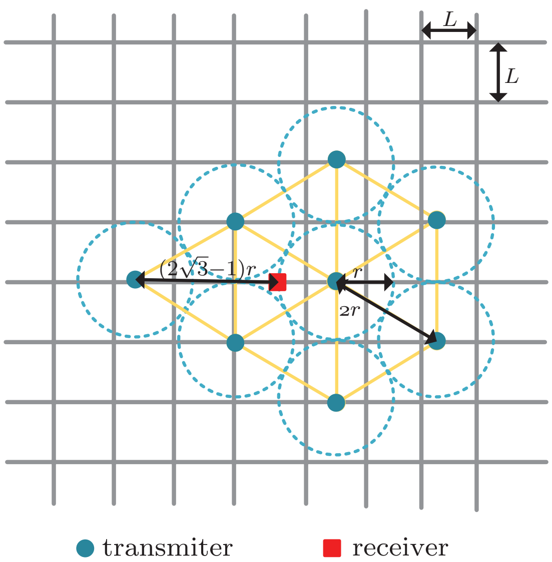

Figure 5 Triangular lattice distribution

Let $SINR_{\mathrm{v}}$ denote the $SINR$ of the received signal at v_0. Since the lower bound of P_{sr} and the upper bounds of I_{ps} and I_{ss} are all obtained, from $SINR_{\mathrm{v}} = P_{\mathrm{sr}}/(I_{\mathrm{ps}} + I_{\mathrm{ss}})$ we can derive the lower bound of the $SINR_{\mathrm{v}}$, which is denoted by ${SINR_{\mathrm{v}}}^{\mathrm{lower}}$.

Theorem 2 For the secondary network, with the vehicle v_0 on a road segment of $Tier\,(\tau_s)$, the channel capacity of V2V transmission is lower-bounded by

$$
\begin{aligned}
{C_{\mathrm{s}}}^{\mathrm{lower}} &= W\mathrm{lb}\left(1 + {SINR_{\mathrm{v}}}^{\mathrm{lower}}\right) \\
&= W\mathrm{lb}\left(1 + \frac{P_{\mathrm{sr}}}{I_{\mathrm{ps}}+I_{\mathrm{ss}}}\right). \quad (14)
\end{aligned}
$$

4 Numerical results

To verify the analytical results obtained in the previous section, a series of simulation have been conducted with MATLAB. We consider a specific city grid of 50 km × 50 km. The power of primary transmitters and secondary transmitters are assumed as 43 dBm and 33 dBm respectively, and the fading factor is 3.

Fig. 6 shows impacts of number and coverage of base stations on the interference introduced by other primary transmitters to the specific primary receiver. It is observed that I_{pp} is an increasing function of

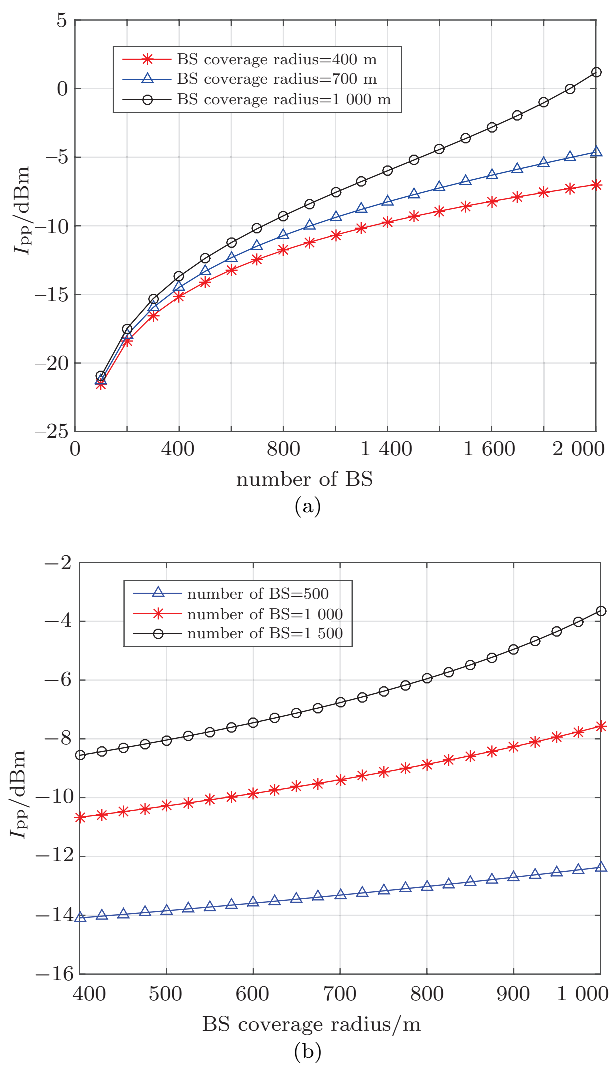

Figure 6 Impact on the interference introduced by other primary transmitters to the specific primary receiver. (a) Number of base stations; (b) coverage of base stations

number and coverage range of base stations respectively. However, the coverage range of base stations has a minimal impact on I_{pp} when the number of base stations is relatively small. This is because of that the denser distribution of base stations means the lager aggregate interference to the specific primary receiver.

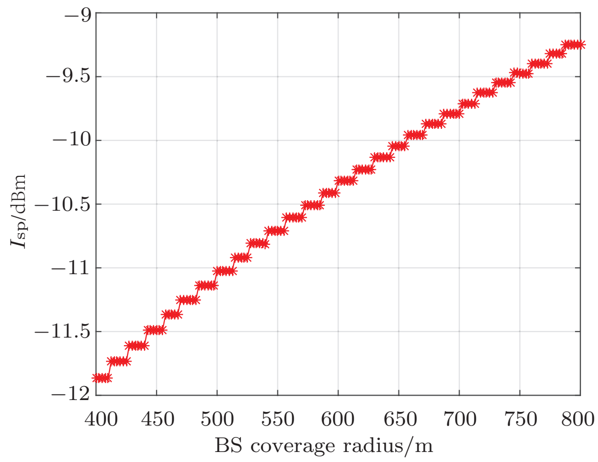

Figure 7 Impact of coverage of base stations on the interference introduced by secondary network to the primary receiver

From Fig. 7, we can see that I_{sp} is approximately a staircase function of the coverage range of base stations. There's equal aggregate interference from the secondary network to the specific primary receiver when the coverage range of base stations is in a certain range. Based on the simulation of I_{pp} and I_{sp}, then we can obtain the lower bound of channel capacity in base station-to-bus transmission as in Fig. 8. It is observed that the lower bound of channel capacity is decreasing when the coverage range and number of base stations increase. This is due to the fact that the total interference will increase while the coverage range and number of base stations increase.

Fig. 9 shows impact of number and coverage of base stations on the interference introduced by primary transmitters to the secondary receiver. It is observed that I_{ps} is an increasing function of number and coverage range of base stations respectively. As the number and coverage range of base stations increase, the density of primary transmitters becomes larger and there's more interference introduced into the secondary network.

As is observed from Fig. 10, the interference introduced by other secondary transmitters to the specific secondary receiver I_{ss} is a decreasing function of length of road segment. I_{ss} is only influenced by the length of road segment and channel propagation environment and independent of base stations. Then the lower bound of channel capacity in V2V transmission can be obtained according to Theorem 2. As shown in Fig. 11, channel capacity of V2V transmission is also a decreasing function of the number and coverage of base stations range.

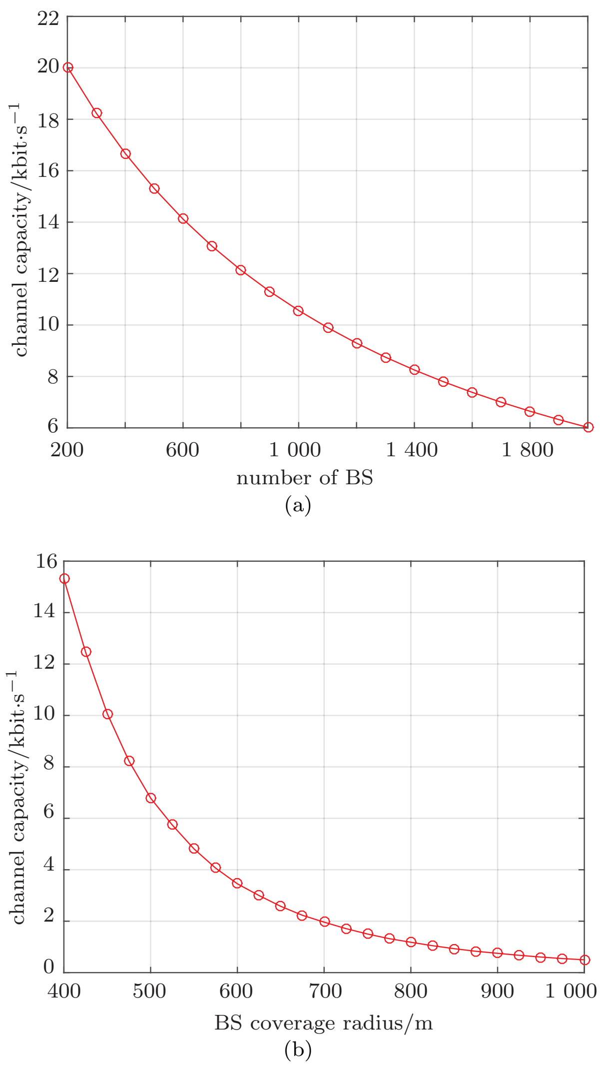

Figure 8 Impact on the lower bound of channel capacity in base station-to-bus transmission. (a) Number of base stations; (b) coverage of base stations

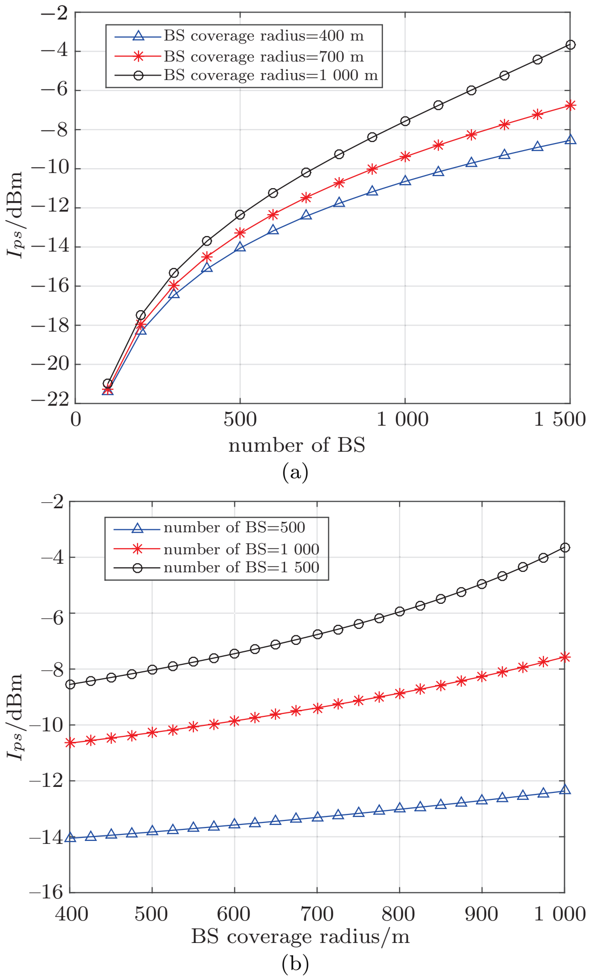

Figure 9 Impact on the interference introduced by primary transmitters to the secondary receiver. (a) Number of base stations; (b) coverage of base stations

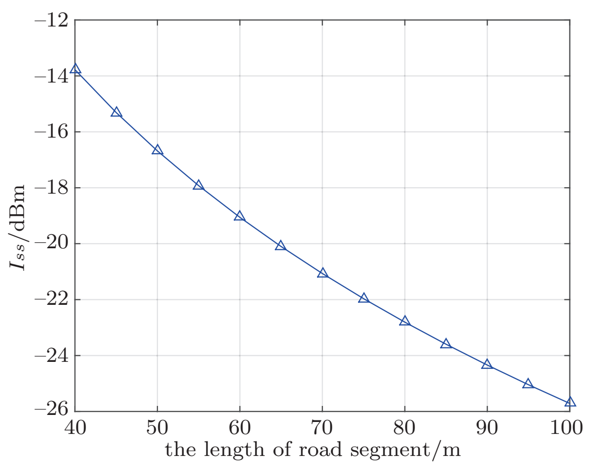

Figure 10 Impact of length of road segment on the interference introduced by other secondary transmitters to the specific secondary receiver

The numerical results validate our analysis of both primary and secondary networks' lower-bound transmission capacities, and illustrate the impacts of BS number, BS coverage and road segment length on interference level and network capacities, which provides guideline for future works.

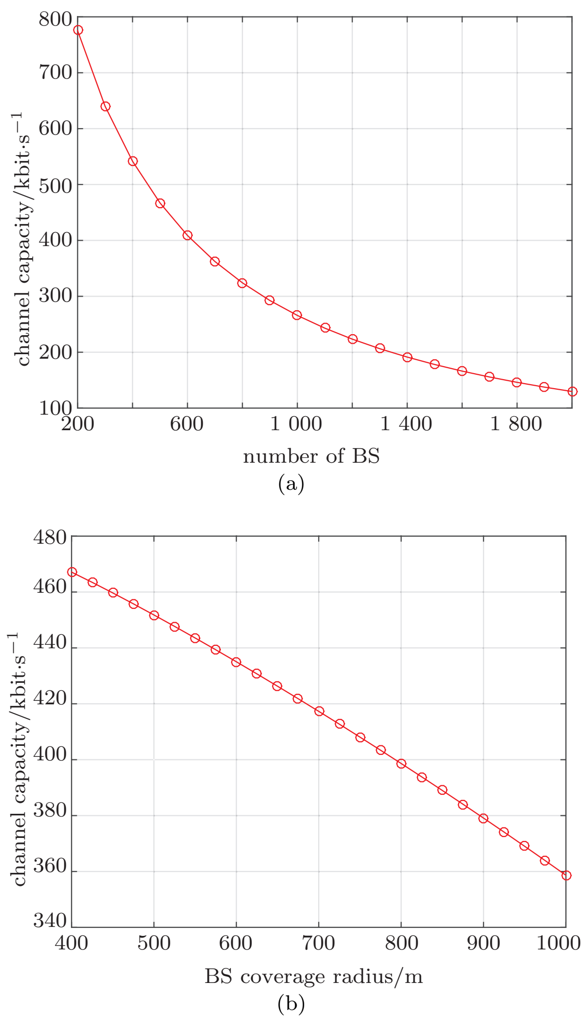

Figure 11 Impact on the lower bound of channel capacity in V2V transmission. (a) Number of base stations; (b) coverage of base stations

5 Conclusion

This paper presents a framework of cellular-based cognitive-radio vehicular Ad hoc networks which consists of a bus Wi-Fi cellular network and a VANET. We consider a scalable urban grid scenario and set a square preservation region to restrict vehicles' interference to primary receivers. The number of street blocks in the preservation region is analyzed. The aggregate interference power from primary and secondary networks are calculated, then the lower-bound of downlink base station-to-bus transmission capacity for primary network and lower-bound of V2V transmission capacity for secondary network are derived respectively. Finally, numerical results provide an insight into the impacts of different network parameters on interference level and network capacities.

References

[1] F. Bai, B. Krishnamachari. Exploiting the wisdom of the crowd: localized, distributed information-centric VANETs [J]. IEEE communications magazine, 2010, 48(5): 138-146.

[2] T. H. Luan, L. X. Cai, J. Chen, et al. VTube: towards the media rich city life with autonomous vehicular content distribution [C]//Sensor, Mesh and Ad hoc Communications and Networks. IEEE, 2011: 359-367.

[3] J. Chen, H. Zhou, N. Zhang, et al. Software defined Internet of vehicles: architecture, challenges and solutions [J]. Journal of communications and information networks, 2016, 1(1): 14-26.

[4] K. Abboud, H. Omar, W. Zhuang. Interworking of DSRC and cellular network technologies for V2X communications: a survey [J]. IEEE transactions on vehicular technology, 2016, 65(12): 9457-9470.

[5] N. Lu, N. Cheng, N. Zhang, et al. Connected vehicles: solutions and challenges [J]. Internet of Things journal IEEE, 2014, 1(4): 289-299.

[6] S. S. Byun, I. Balashingham, A. V. Vasilakos, et al. Computation of an equilibrium in spectrum markets for cognitive radio networks [J]. IEEE transactions on computers, 2014, 63(2): 304-316.

[7] T. Jiang, H. Wang, A. V. Vasilakos. QoE-driven channel allocation schemes for multimedia transmission of priority-based secondary users over cognitive radio networks [J]. IEEE journal on selected areas in communications, 2012, 30(7): 1215-1224.

[8] M. Youssef, M. Ibrahim, M. Abdelatif, et al. Routing metrics of cognitive radio networks: A survey [J]. IEEE communications surveys & tutorials, 2014, 16(1): 92-109.

[9] M. D. Felice, K. R. Chowdhury, L. Bononi. Analyzing the potential of cooperative cognitive radio technology on inter-vehicle communication [C]//IEEE Wireless Days, 2010: 1-6.

[10] K. Fawaz, A. Ghandour, M. Olleik, et al. Improving reliability of safety applications in vehicle Ad hoc networks through the implementation of a cognitive network [C]//IEEE International Conference on Telecommunications, 2010: 798-805.

[11] K. D. Singh, P. Rawat, J. M. Bonnin. Cognitive radio for vehicular Ad hoc networks (CR-VANETs): approaches and challenges [J]. EURASIP journal on wireless communications and networking, 2014(1): 49.

[12] X. He, W. Shi, T. Luo. Survey of cognitive radio VANET [J]. Ksii transactions on internet & information systems, 2014, 8(11): 3837-3859.

[13] S. Chen, J. Hu, Y. Shi, et al. LTE-V: a TD-LTE based V2X solution for future vehicular network [J]. IEEE Internet of Things journal, 2016, PP(99): 1-1.

[14] K. T. Kim, S. K. Oh. Cognitive Ad hoc networks under a cellular network with an interference temperature limit [C]//IEEE International Conference on Advanced Communication Technology, 2008: 879-882.

[15] S. Feizi-Khankandi, F. Ashtiani. Lower and upper bounds for throughput capacity of a cognitive Ad hoc network overlaid on a cellular network [C]//IEEE Wireless Communications and Networking Conference, 2008: 2759-2764.

[16] M. Jiang, X. Fan, F. Zhang, et al. Characterizing on-bus WiFi passenger behaviors by approximate search and cluster analysis [C]//The International Conference on Cloud Computing and Big Data, 2016.

[17] P. Gupta. The capacity of wireless networks [J]. IEEE transactions on information theory, 2000, 46(2): 388-404.

[18] S. P. Weber, X. Yang, J. G. Andrews, et al. Transmission capacity of wireless Ad hoc networks with outage constraints [J]. IEEE transactions on information theory, 2005, 51(12): 4091-4102.

[19] C. Yin, C. Chen, T. Liu, et al. Generalized results of transmission capacities for overlaid wireless networks [C]//IEEE International Conference on Symposium on Information Theory, 2009: 1774-1778.

[20] K. Huang, V. K. N. Lau, Y. Chen. Spectrum sharing between cellular and mobile Ad hoc networks: transmission-capacity trade-off [J]. IEEE journal on selected areas in communications, 2008, 27(7): 1256-1267.

[21] P. Jacquet, P. Muhlethaler. Mean number of transmissions with CSMA in a linear network [C]//IEEE Vehicular Technology Conference Fall, 2010: 1-5.

[22] N. Lu, T. H. Luan, M.Wang, et al. Bounds of asymptotic performance limits of social-proximity vehicular networks [J]. IEEE/ACM transactions on networking, 2014, 22(3): 812-825.

[23] N. Lu, N. Zhang, N. Cheng, et al. Vehicles meet infrastructure: toward capacity-cost tradeoffs for vehicular access networks [J]. IEEE transactions on intelligent transportation systems , 2013, 14(3): 1266-1277.

[24] S. Kostof. The city shaped: urban patterns and mean-

ings through history [M]. New York: Thames and Hudson, 1991.
[25] A. Siksna. The effects of block size and form in North American and Australian city centres [J]. Urban morphology, 1997, 1(1): 19-33.
[26] M. Garetto, E. Leonardi. Restricted mobility improves delay-throughput tradeoffs in mobile Ad hoc networks [J]. IEEE transactions on information theory, 2010, 56(10): 5016-5029.
[27] J. W. Lee, R. R. Mazumdar, N. B. Shroff. Joint resource allocation and base-station assignment for the downlink in CDMA networks [J]. IEEE/ACM transactions on networking, 2006, 14(1): 1-14.
[28] F. Baccelli, B. Laszczyszyn. Stochastic geometry and wireless networks: volume I theory [M]. Boston: Now Publishers Inc. 2009, 3(3-4): 249-449.
[29] M. Haenggi, R. K. Ganti. Interference in large wireless networks [M]. Boston: Now Publishers Inc., 2009, 3(2): 127-248.

About the authors

Xinxin He [corresponding author] is currently a Ph.D. candidate in School of Information and Communication Engineering, Beijing University of Posts and Telecommunications. She received her M.S. degree from Kunming University of Science and Technology in 2013 and B.S. degree from Nanjing University of Posts and Telecommunications in 2009. Her research interests include VANET and cognitive radio networks. (hxx_9000@bupt.edu.cn)

Hang Zhang is currently a M.S. candidate in School of Information and Communication Engineering, Beijing University of Posts and Telecommunications. She received her B.S. degree from Xian Jiaotong University in 2014. Her research interests include Ad hoc networks and cognitive radio networks. (Email: HangZ@bupt.edu.cn)

Tao Luo is Ph.D., IEEE senior member, professor in Beijing University of Posts and Telecommunications. His research interests include mobile communication, cognitive radio networks and WAVE (Wireless Access in Vehicular Environment). (Email: tluo@bupt.edu.cn)

Weisen Shi is currently a Ph.D. candidate in Department of Electrical and Computer Engineering, University of Waterloo. He received M.S. degree from Beijing University of Posts and Telecommunications in 2016, and B.S. degree from Tianjin University in 2013. His research interests include Internet of Vehicles and software defined network. (Email: u46shi@uwaterloo.ca)